OPEN

Microsystems & Nanoengineering (2015) **1,** 15002; doi:10.1038/micronano.2015.2

www.nature.com/micronano

ARTICLE

An implantable microelectrode array for simultaneous L-glutamate and electrophysiological recordings *in vivo*

Wenjing Wei[1,2], Yilin Song[1], Li Wang[1,2], Song Zhang[1,2], Jinping Luo[1], Shengwei Xu[1] and Xinxia Cai[1,2]

L-glutamate, the most common excitatory neurotransmitter in the mammalian central nervous system (CNS), is associated with a wide range of neurological diseases. Because neurons in CNS communicate with each other both electrically and chemically, dual-mode (electric and chemical) analytical techniques with high spatiotemporal resolution are required to better understand glutamate function *in vivo*. In the present study, a silicon-based implantable microelectrode array (MEA) composed of both platinum electrochemical and electrophysiological microelectrodes was fabricated using micro-electromechanical system. In the MEA probe, the electrophysiological electrodes have a low impedance of 0.018 MΩ at 1 kHz, and the electrochemical electrodes show a sensitivity of 56 pA μM^{-1} to glutamate and have a detection limit of 0.5 μM. The MEA probe was used to monitor extracellular glutamate levels, spikes and local field potentials (LFPs) in the striatum of anaesthetised rats. To explore the potential of the MEA probe, the rats were administered to KCl via intraperitoneal injection. K^+ significantly increases extracellular glutamate levels, LFP low-beta range (12–18 Hz) power and spike firing rates with a similar temporal profile, indicating that the MEA probe is capable of detecting dual-mode neuronal signals. It was concluded that the MEA probe can help reveal mechanisms of neural physiology and pathology *in vivo*.

Keywords: MEMS; implantable microelectrode array; glutamate; electrophysiological detection; *in vivo*

Microsystems & Nanoengineering (2015) **1,** 15002; doi:10.1038/micronano.2015.2; Published online: 28 May 2015

INTRODUCTION

L-glutamate, the most common excitatory neurotransmitter in the mammalian central nervous system (CNS), primarily regulates presynaptic and postsynaptic receptors[1–3]. Abnormal transmission of glutamate can cause neurological diseases such as communication dysfunction, cognitive impairments, schizophrenia, Parkinson's disease, stroke and epilepsy[4,5]. Glutamate transformation in excitatory and neurovirulent processes has been studied for decades[6–11]. However, activity in the nervous system includes a complex combination of biochemical and electrical events in space and time[12–14]. Local field potential (LFP) integrates predominantly synaptic input signals from a large population of neurons, whereas spikes or action potentials are output signals of a single neuron[15–17]. Thus, investigating the extracellular electrophysiological signals corresponding to these activities may enable better understanding of glutamatergic processes[16,18].

Several methods have been designed to conduct dual-mode (electric and chemical) neural information recording. Using separate electrodes to examine glutamate and electrophysiological signals within the same preparation has been a commonly employed method[19–22]; however, it is problematic when the separate microelectrodes are not located within the same microenvironment. Several reports delivered external glutamate or drugs that could affect glutamate release into the rat brain and recorded only electrophysiological signal changes[23–28]; however, this method can serve in only a limited capacity for glutamate change is not quantitative. Studying dual-mode activity by randomly dividing rats into groups for electrophysiological and neurotransmitter monitoring is another method that has been pursued[29]. When using this method, it is important to consider the sample individual difference. Consequently, the development of a novel electrode capable of simultaneously detecting electrochemical and electrophysiological signals *in vivo* is of great significance and should enable the monitoring of glutamatergic activity in living systems.

For this purpose, an implantable silicon microelectrode array (MEA) probe incorporating both Pt electrophysiological and glutamate recording sites was fabricated using micro-electromechanical systems (MEMS) method. In this approach, the microelectrode arrangement can be flexibly designed and precisely controlled for use in dual-mode *in vivo* recording[30–33]. We modified the MEA probe with Pt nanoparticles and 1,3-phenylenediamine (mPD) to improve electrical performance. We then implanted the MEA probe into the striatum of anaesthetised rats and, following intraperitoneal (i.p.) administration of KCl, examined extracellular glutamate, LFP and spike activity. The results demonstrated the ability of the implantable MEA to simultaneously record dynamic changes in L-glutamate and neural electrical activity *in vivo*.

MATERIALS AND METHODS

Reagents and apparatus

Glutamate oxidase (GluOx) was obtained from Yamasa Corporation, Japan. Ascorbic acid (AA, ≥99%), 3,4-dihydroxyphenylacetic acid (DOPAC, ≥98%) and 5-hydroxytryptamine (5-HT, 99%) were obtained from Alfa Aesar Corporation, USA. Dopamine (DA, ≥99%) was obtained from Acros Organics, Belgium. Saline (0.9% NaCl) was purchased from the Shuanghe Company, China. Urethane (≥98%) was obtained from Sinopharm Chemical Reagent Co., Ltd, China. mPD (≥99%) was purchased from Aldrich, USA. Bovine serum albumin (BSA, ≥99%) was purchased from Amresco,

[1]State Key Laboratory of Transducer Technology, Institute of Electronics, Chinese Academy of Sciences, Beijing 100190, China; [2]University of Chinese Academy of Sciences, Beijing 100049, China

Correspondence: Xinxia Cai (xxcai@mail.ie.ac.cn)

Received: 1 December 2014; Revised: 3 April 2015; Accepted: 6 April 2015

USA. Glutaraldehyde solution (GA, 25%) and L-glutamate sodium (>98%) were purchased from Shanghai Chemical Reagent Company, China. Phosphate-buffered saline (PBS, 0.1 M, Na_2HPO_4-NaH_2PO_4-KCl, pH 7.4) was prepared from a PBS tablet (Sigma) with deionised water. Water was purified through a Michem ultrapure water apparatus, China (resistivity >18 MΩ).

The KCl solution (100 mM, 1 mL kg^{-1}) used for i.p. administration was prepared in normal saline and sonicated for 5 min at 37 °C to ensure complete dissolution. The remaining solutions were prepared in PBS (0.1 mM, pH 7.4). DOPAC, DA, 5-HT and AA solutions were prepared just before use because of their propensity to decompose over time.

All electrochemical measurements were performed on a Gamry electrochemical workstation (Gamry Reference 600, Gamry Instruments, USA). Electrophysiological signals were recorded using an integrated 16-channel filter amplifier and data acquisition system (USB-ME16-FAI-System, Multi-Channel Systems, Germany).

MEA probe fabrication and modification

An implantable MEA probe was created using silicon-on-insulator substrates (SOI, 30 μm Si/2 μm SiO_2/600 μm Si) by MEMS method using the following steps. (i) The front side of the SOI (30 μm Si) was coated with 0.5 μm of silicon dioxide by wet oxidation. (ii) The electrophysiology and glutamate recording sites, lead wires and bonding pads in the MEA probe were patterned by photolithography (positive photoresist AZ1500, 1 μm thick), Pt/Ti (250 nm/30 nm thick) sputtering and lift-off methods. (iii) A final silicon nitride (0.8 μm) layer was deposited via plasma enhanced chemical vapour deposition (PECVD, 300 °C) to provide insulation. Windows to the recording points and bonding pads were opened using reactive-ion etching (RIE). (iv) The MEA probe shape was defined by deep RIE from the top of the 30 μm thick silicon layer down to the buried oxide. (v) A thick picein wax (Kunlun 80#, Oil Refining Chemical General Factory Chinese Oil Yumen Oilfield Company, China) was spun on the wafer front side for protection, and KOH (30%) was used to wet etch the full 600 μm span of backside silicon down to the buried oxide. In this way, the individual MEA probe was released from the underlying silicon substrate. The picein wax was washed out using negative photoresist developer and fuming nitric acid. The imbedded oxide was smashed and removed by ultrasonic cleaning in pure water with a power of 40 W for 2 min.

The MEA probe consisted of a single 7 mm-long shank and was 30 μm × 343 μm in cross section. Along the shank, there was a linear array of 14 microelectrode sites that alternated between being round (diameter = 15 μm) and rectangular (60 μm × 125 μm) for transduction of electrophysiological and amperometric signals, respectively (Figure 1a). The centre-to-centre site separation was 170 μm between two adjacent electrochemical sites, 80 μm between two adjacent electrophysiological sites, and 150 μm between an electrophysiological site and an adjacent electrochemical site. Maintaining a 50–200 μm distance between recording sites was reasonable as a shorter inter-electrode separation could result in possible cross-talk artefacts, whereas a larger separation would miss cross-correlations between neuron pairs[18,34]. The MEA probe was wire bonded to a printed circuit board (PCB) holder for handling and connecting to the recording equipment (Figure 1b). The bonding pads, bonding wires and metal lines on the PCB were embedded in silicone rubber (Nanda 705#, Liyang Kangda Chemical Co. Ltd., China) for the purpose of mechanically protecting and electrically isolating the connections. The assembled MEA probe could then be implanted into a rat's brain (Figure 1c).

To reduce the impedance of the electrophysiological electrode, Pt nanoparticles were electrodeposited on the round microelectrodes using chloroplatinic acid (48 mM) and lead acetate (4.2 mM) in a 1:1 mixed solution at −1.0 V opposite a Pt electrode for 60 s (Figure 1a). The adsorption and underpotential deposition of lead ions in the electrodeposited platinum led to changes in morphology and crystal size of the Pt nanostructures[35].

Cross-linked covalent binding through glutaraldehyde was employed to immobilise the GluOx in the Pt electrochemical recording site. Using a three-dimensional micro-operator, the MEA probe was inserted into a glass capillary filled with a mixed solution of GluOx (1%), BSA (1%) and GA (0.125%), and the probe insertion length was precisely controlled. Under microscopic guidance, when the first glutamate recording site was covered with GluOx solution, the probe was drawn out of the solution. Thus, only the first site was exposed to GluOx (Supplementary Figure S1).

MPD was electrochemically polymerised on the eight electrochemical electrodes (every area equalled 60 × 125 μm^2) at a potential of +0.6 V versus an Ag|AgCl reference electrode for 15 min in a 5 mM mPD solution prepared in PBS.

Electrochemical characterisation

The impedance spectrum of the electrophysiological microelectrodes with and without Pt nanoparticles was evaluated using electrochemical impedance spectroscopy (EIS) in an electrochemical workstation. The MEA probe and an Ag|AgCl reference electrode were placed in a PBS solution. The impedance was assessed over a frequency range of 0.1 Hz to 100 kHz at a voltage level of +0.02 V.

Electrochemical detection of glutamate by the sensor occurs as follows. First, glutamate is converted by GluOx to hydrogen peroxide (H_2O_2), α-ketoglutarate and NH_3. Next, H_2O_2 is electrochemically oxidised on the surface of the Pt electrode, thereby providing a current signal proportional to the glutamate concentration. Calibrations were carried out in PBS buffer with a two-electrode configuration, the applied potential was held at +0.7 V *vs*. Ag|AgCl; this value is typically used for H_2O_2 detection. A 5 × 2 mm^2 stir bar was added to the PBS and the solution was stirred slowly to prevent the formation of a vortex in the solution. The sensitivity and detection limit were determined by a stepwise addition of 5 μM to 30 μM glutamate into the buffer. There are several common neurotransmitters that can cause interference in brain extracellular fluid (ECF), including DOPAC (≈20 μM in ECF), AA (250–500 μM in ECF), DA (≤100 nM in ECF) and 5-HT (≤1 μM in ECF)[36]. To investigate the selectivity of the electrode, the responses of the GluOx-coated microelectrodes and mPD–GluOx-modified microelectrodes to the above-listed interferences were compared. Stock solutions of the interfering molecules were diluted into buffer to produce the following solutions: 20 μM DOPAC, 1 μM DA, 1 μM 5-HT and 250 μM AA.

In vivo experiments

For *in vivo* testing, male Sprague–Dawley rats (270 g) were individually anaesthetised with urethane (1.4 g kg^{-1}, i.p.), and an MEA probe was

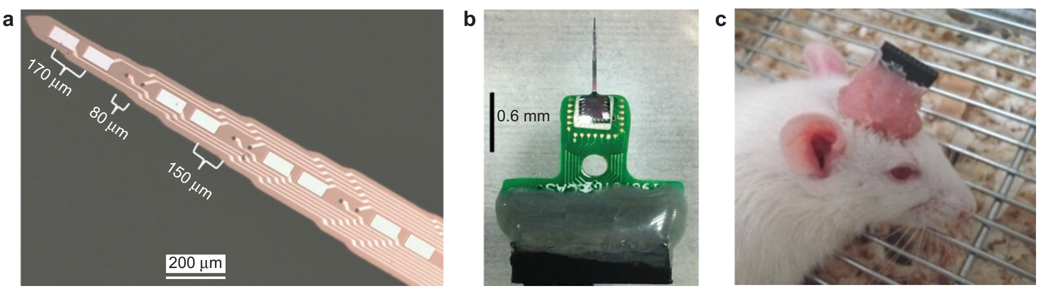

Figure 1 (**a**) Photomicrograph of the MEA probe tip. Along the shank, the microelectrodes alternated between being round (diameter = 15 μm) and rectangular (60 μm × 125 μm) in shape to enable the recording of electrophysiological and amperometric signals, respectively. Pt nanoparticles were deposited on the electrophysiological electrodes. (**b**) The MEA probe was assembled into a PCB holder. (**c**) The assembled MEA probe implanted in a freely moving rat.

 doi:10.1038/micronano.2015.2

implanted into the striatum of each animal (AP: +1.0 mm, ML: −2.5 mm, DV: −5.0 mm). A homemade Ag|AgCl reference electrode (an Ag wire on which AgCl was electrodeposited) was placed into the cortex. An earth wire, used as a ground, was attached to one of the support screws during recording.

The implanted MEA probe was connected to the electrophysiological recording system and the electrochemical workstation. The six-channel electrophysiological signals were sampled simultaneously at a rate of 25 kHz. A low pass filter was applied at 100 Hz to view the LFP, and a high pass filter was applied at 500 Hz to view the neural spikes. Such broadband recordings allow for the simultaneous investigation of spikes and LFP. Power spectral densities of recorded LFPs were calculated in MATLAB using the correlation function and Fourier transform function (Hamming window, 2 s window, 1 s steps). The glutamate signals were recorded using constant amperometry responses. The working potential was held at +0.7 V *vs.* the Ag|AgCl reference wire. Glutamate recordings were not made until at least 30 min had elapsed after probe insertion to allow for glutamate levels to equilibrate, and signals were recorded at 0.1 s intervals. The entire experiment was conducted inside a Faraday cage. All of the procedures detailed above complied with the guidelines of the State Scientific and Technological Commission for the care and use of laboratory animals.

RESULTS AND DISCUSSION

Impedance test

Figure 2 details the electrochemical impedance spectrum of the electrophysiological microelectrodes before and after Pt nanoparticles were deposited on them. The nanoparticles possessed large surface areas[37] and therefore increased the geometrical surface area of the electrode, reducing electrode impedance. In using Pt nanoparticles, the mean impedance of the microelectrodes at 1 kHz decreased from 0.33 to 0.018 MΩ ($n = 6$) (Figure 2), which is a desirable range for electrical neural recording.

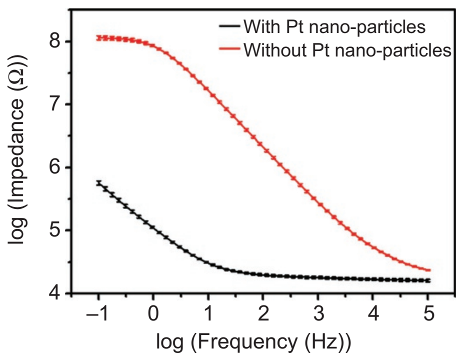

Figure 2 Impedance spectra of electrophysiological microelectrodes before and after Pt nanoparticles were deposited on them. The frequency range was 0.1–100 kHz, and the voltage level was +0.02 V *vs.* Ag|AgCl reference electrode.

Glutamate calibration

Prior to the surgical procedures, each GluOx–mPD-modified recording site was characterised for its sensitivity to glutamate. The microelectrode exhibited a sensitivity of 56 pA μM^{-1} to L-glutamate and had a relative coefficient of 0.995 over a range of 5–30 μM (Figure 3a and b). The detection limit was 0.5 μM when the signal-to-noise ratio was greater than 3. These are viable conditions for *in vivo* recording as basal glutamate concentrations

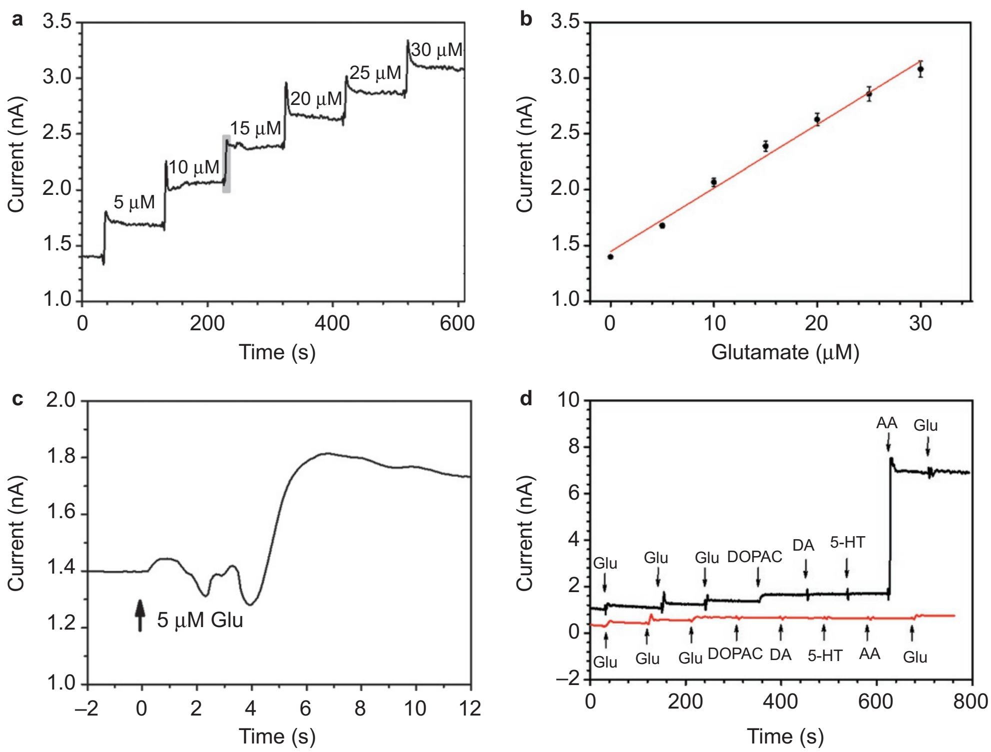

Figure 3 Performance of the glutamate microelectrode, the applied potential was held at +0.7 V vs. Ag|AgCl. (**a**) mPD–GluOx microelectrode response to varying concentrations of glutamate. (**b**) Plot of current vs. glutamate concentration (n = 3). The sensitivity was 56 pA μM^{-1}, R = 0.995. (**c**) Enlargement of selected section from curve (**a**). (**d**) Performance of GluOx-coated microelectrodes without (top trace) and with (bottom trace) mPD electropolymerisation. Arrows indicate the additions of various substances: L-glutamate (3 μM, three times), DOPAC (20 μM), DA (1 μM), 5-HT (1 μM), AA (250 μM), and another addition of L-glutamate (3 μM), numbers in the parentheses are the final concentration.

of SD rats ranges between 1.2 μM and 8.1 μM[4,38,39]. As shown in Figure 3c, the response time of the electrode was shorter than 8 s after the addition of 5 μM L-glutamate. When the glutamate level was changed to a lower concentration, the response time was also shorter than 8 s (Supplementary Figure S2). Figure 3d illustrates the typical amperometric responses to glutamate, DOPAC, DA, 5-HT and AA of the GluOx-coated electrode (with and without mPD electropolymerisation) in the on-line detection system at a working potential of +0.7 V. The results demonstrated that the interference conditions could not produce measurable responses in the mPD–GluOx-modified channel, which convincingly indicates that measurements of glutamate were essentially interference-free with respect to these electroactive species.

The stability of the glutamate microelectrode can be illustrated by following observations: the sensitivity to glutamate decreased to 97.60 ± 3.08% (n = 3) after 2 h of recording *in vivo*, and it decreased to 46.32 ± 5.08% (n = 3) after 9 h of recording *in vivo*. The coefficient of variation for glutamate measurements acquired under the same *in vivo* conditions was 2.92% (n = 3); measurements of reproducibility were performed at different time points using a single rat. The glutamate microelectrode maintained 93.39 ± 2.71% (n = 3) of its original sensitivity after being stored at 4 °C for 26 days.

The cross-linked enzyme (GluOx) layer that was coated on the microelectrode had a thickness of 140–180 nm, as measured by a step profiler, and there was evidence that the subsequent electropolymerisation of mPD produced a thin, self-sealing, insulating polymer film with thickness of ~15 nm[40] on the microelectrode surface (Supplementary Figure S3). Poly (mPD) film possesses excellent interference-rejection characteristic as it can prevent larger molecules such as AA, DA, 5-HT and DOPAC from reaching the microelectrode surface[41]. Smaller molecules, such as H_2O_2, are still able to pass through the film. The use of a poly (mPD) film also serves as a method of immobilising GluOx and protecting the microelectrode surface from fouling. L-glutamate is not able to penetrate a poly (mPD) film; however, when it comes into contact with the GluOx molecules located at the polymer|electrolyte interface, it can be catalysed to produce H_2O_2. The resultant H_2O_2 can pass through the poly (mPD) film and is oxidised on the microelectrode surface. Thus, the microelectrode current signal that is produced is proportional to L-glutamate concentration.

Concurrent recordings of striatum glutamate overflow and electrophysiological changes

An MEA probe was implanted into the striatum of an anaesthetised rat. To explore the capability of the MEA probe at detecting dynamic changes in glutamate and electrophysiological signals, KCl (100 mM, 1 mL kg^{-1}) was administered to the rat through i.p. injection.

Figure 4a shows the influence of KCl on striatum glutamate levels. The basal striatum glutamate concentration was 3.01 ± 1.27 μM before KCl injection. After 1.23 ks of KCl injection, the glutamate increased to 4.67 ± 0.82 μM, and this increased concentration lasted for 0.75 ks (Figure 4a). Following this, there was a gradual return to baseline values. The high concentration of K^+ caused massive depolarisation of neurons and consequently led to the release of glutamate from vesicular, cytosolic pools and astrocytes[38]. The average striatum glutamate release stimulated by K^+ was calculated to be ~1.66 μM.

Prior to KCl stimulation, the striatum LFP exhibited slow-wave activity (0.1–4 Hz) (Figure 4b), and the spike exhibited low firing rates and non-bursting activity (Figure 4d and e). These conditions are characteristics of urethane anaesthesia. The extracellular recorded spikes were classified into two different types according to their waveforms (Figure 4g). The type 1 spike, which appeared

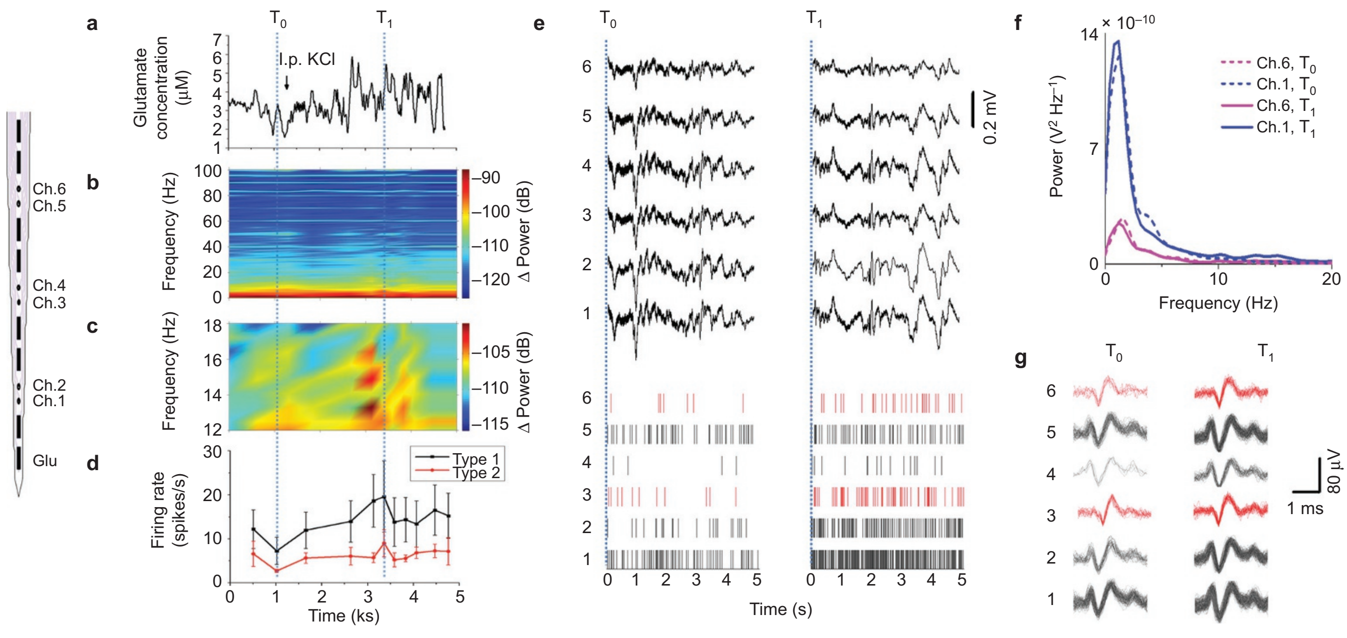

Figure 4 I.p. injection of KCl (100 mM, 1 mL kg^{-1}) evokes changes in glutamate concentration and electrophysiological activity, which were simultaneously recorded along an MEA probe implanted into the striatum of an anaesthetised rat. The left panel shows the marked recording sites in the MEA probe. (**a**) Variation in glutamate concentration elicited by i.p. injection of KCl (indicated by an arrow). The power spectrogram of LFP recorded in Channel 1 (Ch. 1). (**b**) from 0 to 100 Hz and (**c**) from 12 to 18 Hz. (**d**) The corresponding mean firing rates of different type spikes. The same time epochs were used in (**a**), (**b**), (**c**) and (**d**). (**e**) LFPs (upper) and spike trains (lower) recorded at 0.26 ks before (T_0) and 2.08 ks after (T_1) KCl injection. (**f**) Power spectral densities of the LFPs from Ch. 1 and Ch. 6 in (**e**). (**g**) Spike waveforms recorded in each recording channel before (T_0) and after (T_1) KCl injection. The spike colours are the same as in (**d**), (**e**) and (**f**). T_0 and T_1 indicate the times at which the LFPs and spike traces were obtained.

 doi:10.1038/micronano.2015.2

in microelectrode channels 1, 2, 4 and 5, was fired with a 0.4 ms positive protrusion before the 0.4 ms negative phase and was followed with a positive phase of 0.6 ms. The type 2 spike, which appeared in microelectrode channels 3 and 6, was initially fired with a negative phase of 0.4 ms and was followed with a positive phase of 0.6 ms.

After KCl stimulation, the released glutamate led to a decrease in rheobase and depolarisation voltage and compressed the range of recruitment threshold current[42], thereby exciting the glutamate-exposed neurons. Therefore, the firing rates of both types of spike and the LFP low-beta (12–18 Hz) activity (Figure 4c), which represents the potentiation of excitatory neurotransmission between co-activated neuronal networks, were increased by glutamate augmentation. In the case of the type 1 spike, the firing rate increased from 7.24 ± 3.06 spikes s^{-1} at 0.26 ks before KCl injection (T_0) to 19.60 ± 8.07 spikes s^{-1} at 2.08 ks after of KCl injection (T_1). The firing rate of the type 2 spike increased from 2.72 ± 0.35 spikes s^{-1} at T_0 to 9.01 ± 3.10 spikes s^{-1} at T_1. The duration of the switch in LFP power and spike firing rates paralleled the time course of KCl-induced extracellular glutamate fluctuation. To validate the dual-mode results, glutamate and electrophysiological signals were obtained from the brain of a dead rat, which should not produce any biochemical or bioelectrical signals (Supplementary Figure S4).

Multichannel signals reflect the spatial composition distribution in a recorded brain region. Figure 4f shows that the LFP power spectral density obviously changed with respect to the positioning of recording sites, which indicates that the striatum has inputs from different encephalic regions[43]. In Figure 4g, two types of spike waveform are indicated, revealing that two classes of neurons were recorded for each neuronal type generated identical action potentials[44]. These results provided evidence that different glutamate input and output pathways exist in the striatum.

In the present study, the potential of using a dual-mode implantable MEA as a research tool *in vivo* was explored. The MEA probe presents several advantages over alternative neural recording methods. First, due to its dual-mode design, a lesser degree of brain damage is caused when using this probe, which may result in the detection of more physiologically relevant extracellular glutamate pools and electrophysiological signals. Second, the sensor is able to simultaneously detect second-to-second changes in glutamate and electrophysiological signals. Finally, the microelectrode sites have precise spatial definition, which can be an advantage when studying layered brain structures. With the real-time multichannel dual-mode signals that can be acquired by the MEA probe, the spatiotemporal relationships between neurons that are embedded in different regions of brain tissue can be thoroughly analysed.

CONCLUSION

Using MEMS, we created a novel implantable MEA probe that can produce simultaneous measurements of glutamate, LFP and spike activities across multiple spatial locations in the rat brain. Recordings from the MEA probe that were taken in the striatum of urethane-anaesthetised rats revealed spatiotemporal K^+-evoked dual-mode signal changes, which indicates that the MEA probe is useful for investigating neural dynamics *in vivo*. In the future, we intend to apply this biosensor technology to analyse neurologic dysfunction in a rat model of Parkinson's disease.

ACKNOWLEDGEMENTS

This work was sponsored by the Major National Scientific Research Plan (Grant Nos. 2011CB933202 and 2014CB744605), the NSFC (Grant Nos. 61125105 and 61471342), the Beijing Science and Technology Plan (Grant Nos. Z141100000214002 and Z141102003414014) and the Key Programs of the Chinese Academy of Sciences (Grant No. KJZD-EW-L11-2).

COMPETING INTERESTS

The authors declare no conflict of interest.

REFERENCES

1 Quintero JE, Pomerleau F, Huettl P *et al.* Methodology for rapid measures of glutamate release in rat brain slices using ceramic-based microelectrode arrays: basic characterization and drug pharmacology. *Brain Research* 2011; **1401**: 1–9.
2 Zilkha E, Obrenovitch TP, Koshy A *et al.* Extracellular glutamate: on-line monitoring using microdialysis coupled to enzyme-amperometric analysis. *Journal of Neuroscience Methods* 1995; **60**: 1–9.
3 Burmeister JJ, Pomerleau F, Palmer M *et al.* Improved ceramic-based multisite microelectrode for rapid measurements of L-glutamate in the CNS. *Journal of Neuroscience Methods* 2002; **119**: 163–171.
4 Konradsson-Geuken A, Wu HQ, Gash CR *et al.* Cortical kynurenic acid bi-directionally modulates prefrontal glutamate levels as assessed by microdialysis and rapid electrochemistry. *Neuroscience* 2010; **169**: 1848–1859.
5 Muthuswamy J, Okandan M, Jackson N. Single neuronal recordings using surface micromachined polysilicon microelectrodes. *Journal of Neuroscience Methods* 2005; **142**: 45–54.
6 Sugahara M, Asai S, Zhao H *et al.* Extracellular glutamate changes in rat striatum during ischemia determined by a novel dialysis electrode and conventional microdialysis. *Neurochemistry International* 2001; **39**: 65–73.
7 Tian F, Gourine AV, Huckstepp RT *et al.* A microelectrode biosensor for real time monitoring of L-glutamate release. *Analytica Chimica Acta* 2009; **645**: 86–91.
8 Albery WJ, Boutelle MG, Galley PT. The dialysis electrode: a new method for in vivo monitoring. *Journal of the Chemical Society, Chemical Communications* 1992; **12**: 900.
9 Fillenz M. Physiological release of excitatory amino acids. *Behavioural Brain Research* 1995; **71**: 51–67.
10 Centonze D, Gubellini P, Usiello A *et al.* Differential contribution of dopamine D2S and D2L receptors in the modulation of glutamate and GABA transmission in the striatum. *Neuroscience* 2004; **129**: 157–166.
11 Agnesi F, Blaha CD, Lin J *et al.* Local glutamate release in the rat ventral lateral thalamus evoked by high-frequency stimulation. *Journal of Neural Engineering* 2010; **7**: 26009.
12 Song Y, Lin N, Liu C *et al.* A novel dual mode microelectrode array for neuroelectrical and neurochemical recording *in vitro*. *Biosensors and Bioelectronics* 2012; **38**: 416–420.
13 Shoham S, O'Connor DH, Sarkisov DV *et al.* Rapid neurotransmitter uncaging in spatially defined patterns. *Nature Methods* 2005; **2**: 837–843.
14 LeChasseur Y, Dufour S, Lavertu G *et al.* A microprobe for parallel optical and electrical recordings from single neurons *in vivo*. *Nature Methods* 2011; **8**: 319–325.
15 Foffani G, Ardolino G, Egidi M *et al.* Subthalamic oscillatory activities at beta or higher frequency do not change after high-frequency DBS in Parkinson's disease. *Brain Research Bulletin* 2006; **69**: 123–130.
16 Waldert S, Lemon RN, Kraskov A. Influence of spiking activity on cortical local field potentials. *Journal of Physiology* 2013; **591**: 5291–5303.
17 Li Z, Ouyang G, Yao L *et al.* Estimating the correlation between bursty spike trains and local field potentials. *Neural Networks* 2014; **57**: 63–72.
18 Johnson MD, Franklin RK, Gibson MD *et al.* Implantable microelectrode arrays for simultaneous electrophysiological and neurochemical recordings. *Journal of Neuroscience Methods* 2008; **174**: 62–70.
19 Dash MB, Douglas CL, Vyazovskiy VV *et al.* Long-term homeostasis of extracellular glutamate in the rat cerebral cortex across sleep and waking states. *Journal of Neuroscience* 2009; **29**: 580–589.
20 Naylor E, Aillon DV, Gabbert S *et al.* Simultaneous real-time measurement of EEG/EMG and L-glutamate in mice: a biosensor study of neuronal activity during sleep. *Journal of Electroanalytical Chemistry* 2011; **656**: 106–113.
21 Ueda Y, Doi T, Tokumaru J *et al.* Kindling phenomena induced by the repeated short-term high potassium stimuli in the ventral hippocampus of rats: on-line monitoring of extracellular glutamate overflow. *Experimental Brain Research* 2000; **135**: 199–203.
22 Gruss M, Bredenkotter M, Braun K. N-methyl-D-aspartate receptor-mediated modulation of monoaminergic metabolites and amino acids in the chick forebrain: an *in vivo* microdialysis and electrophysiology study. *Journal of Neurobiology* 1999; **40**: 116–135.
23 Mulder AB, Manshanden I, Vos PE *et al.* Modifications in glutamatergic transmission after dopamine depletion of the nucleus accumbens. A combined *in vivo/in vitro* electrophysiological study in the rat. *Neuroscience* 1996; **72**: 1009–1021.
24 Cooper DC, White FJ. L-type calcium channels modulate glutamate-driven bursting activity in the nucleus accumbens *in vivo*. *Brain Research* 2000; **880**: 212–218.

25 Klukowski G, Harley CW. Locus coeruleus activation induces perforant path-evoked population spike potentiation in the dentate gyrus of awake rat. *Experimental Brain Research* 1994; **102**: 165–170.
26 Sakata Y, Fujioka T, Chowdhury GMI *et al*. *In vivo* electrical activity of brainstem neurons in fetal rats during asphyxia. *Brain Research* 2000; **871**: 271–280.
27 Kida I, Smith AJ, Blumenfeld H *et al*. Lamotrigine suppresses neurophysiological responses to somatosensory stimulation in the rodent. *Neuroimage* 2006; **29**: 216–224.
28 Herreras O, Largo C, Ibarz JM *et al*. Role of neuronal synchronizing mechanisms in the propagation of spreading depression in the *in-vivo* hippocampus. *Journal of Neuroscience* 1994; **14**: 7087–7098.
29 Wang D, Liu X, Qiao D. Modulatory effect of subthalamic nucleus on the development of fatigue during exhausting exercise: an *in vivo* electrophysiological and microdialysis study in rats. *Journal of Sports Science and Medicine* 2012; **11**: 286–293.
30 Frey O, Holtzman T, McNamara RM *et al*. Enzyme-based choline and L-glutamate biosensor electrodes on silicon microprobe arrays. *Biosensors and Bioelectronics* 2010; **26**: 477–484.
31 Chang L, Liu C, He Y *et al*. Small-volume solution current-time behavior study for application in reverse iontophoresis-based non-invasive blood glucose monitoring. *Science China Chemistry* 2011; **54**: 223–230.
32 Lee K, He J, Clement R *et al*. Biocompatible benzocyclobutene (BCB)-based neural implants with micro-fluidic channel. *Biosensors and Bioelectronics* 2004; **20**: 404–407.
33 Grand L, Pongrácz A, Vázsonyi É *et al*. A novel multisite silicon probe for high quality laminar neural recordings. *Sensors and Actuators A: Physical* 2011; **166**: 14–21.
34 Xu C, Lemon W, Liu C. Design and fabrication of a high-density metal microelectrode array for neural recording. *Sensors and Actuators A: Physical* 2002; **96**: 78–85.
35 Plowman BJ, Abdelhamid ME, Ippolito SJ *et al*. Electrocatalytic and SERS activity of Pt rich Pt-Pb nanostructures formed via the utilisation of in-situ underpotential deposition of lead. *Journal of Solid State Electrochemistry* 2014; **18**: 3345–3357.
36 Wei WJ, Song YL, Shi WT *et al*. A high sensitivity MEA probe for measuring real time rat brain glucose flux. *Biosensors and Bioelectronics* 2014; **55**: 66–71.
37 Wang J, Su M-Y, Qi J-Q *et al*. Sensitivity and complex impedance of nanometer zirconia thick film humidity sensors. *Sensors and Actuators B: Chemical* 2009; **139**: 418–424.
38 Yu Y, Liu X, Jiang D *et al*. [C3(OH)2mim][BF4]-Au/Pt biosensor for glutamate sensing *in vivo* integrated with on-line microdialysis system. *Biosensors and Bioelectronics* 2011; **26**: 3227–3232.
39 Day BK, Pomerleau F, Burmeister JJ *et al*. Microelectrode array studies of basal and potassium-evoked release of L-glutamate in the anesthetized rat brain. *Journal of Neurochemistry* 2006; **96**: 1626–1635.
40 Killoran SJ, O'Neill RD. Characterization of permselective coatings electrosynthesized on Pt-Ir from the three phenylenediamine isomers for biosensor applications. *Electrochimica Acta* 2008; **53**: 7303–7312.
41 Mattinson CE, Burmeister JJ, Quintero JE *et al*. Tonic and phasic release of glutamate and acetylcholine neurotransmission in sub-regions of the rat prefrontal cortex using enzyme-based microelectrode arrays. *Journal of Neuroscience Methods* 2011; **202**: 199–208.
42 Torres-Torrelo J, Rodriguez-Rosell D, Nunez-Abades P *et al*. Glutamate modulates the firing rate in oculomotor nucleus motoneurons as a function of the recruitment threshold current. *Journal of Physiology* 2012; **590**: 3113–3127.
43 Berke JD. Fast oscillations in cortical-striatal networks switch frequency following rewarding events and stimulant drugs. *European Journal of Neuroscience* 2009; **30**: 848–859.
44 Buzsaki G. Large-scale recording of neuronal ensembles. *Nature Neuroscience* 2004; **7**: 446–451.

Supplementary information for this article can be found on the *Microsystems & Nanoengineering* website (http://www.nature.com/micronano).

doi:10.1038/micronano.2015.2